Babol University of Medical Sciences
IJMCM
International Journal of Molecular and Cellular Medicine
p-ISSN: 2251-9637 o-ISSN: 2251-9645
Cellular and Molecular Biology Research Center

Extracellular Signal-Regulated Kinase Inhibitor SCH772984 Augments the Anti-Cancer Effects of Gemcitabine in Nanoparticle Form in Pancreatic Cancer Models

Gauthami G Nair[1*], Elena D Linster[1], Priyanka Ray[2], Mohiuddin A Quadir[2], Katie M Reindl[1]

1. Department of Biological Sciences, NDSU, Fargo, North Dakota, U.S.A.

2. Department of Coatings and Polymeric Materials, NDSU, Fargo, North Dakota, U.S.A.

Article type: **Original Article**

Received: 2024.04.26
Revised: 2024.07.15
Accepted: 2024.07.27

ABSTRACT

Pancreatic ductal adenocarcinoma (PDAC) is a lethal disease with a poor response to the limited treatment options currently available. Hence, there is a need to identify new agents that could enhance the efficacy of existing treatments. This study investigated a combination therapy using gemcitabine (GEM) and SCH772984, an extracellular signal-regulated kinase (ERK) inhibitor, in both free form and nanoparticle-encapsulated form for PDAC treatment. Cell viability and Matrigel growth assays were used to determine the anti-proliferative and cytotoxic effects of GEM and SCH772984 on PDAC cells. Additionally, western blotting was used to determine the degree to which SCH772984 engaged ERK in PDAC cells. Lastly, immunohistochemistry and hematoxylin and eosin (H&E) staining were used to determine how GEM and SCH772984 affected expression of Ki-67 cell proliferation marker in PDX (patient derived xenograft) PDAC tissues. PDAC cell lines (MIA PaCa-2 and PANC-1) treated with the combination of free GEM and SCH772984 showed reduction in cell viability compared to cells treated with free GEM or SCH772984 administered as a single agent. Encapsulated forms of GEM and SCH772984 caused a greater reduction in cell viability than the free forms. Interestingly, co-administration of GEM and SCH772984 in separate nanoparticle (NP) systems exhibited the highest reduction in cell viability. Western blotting analysis confirmed ERK signaling was inhibited by both free and encapsulated SCH772984. Importantly, GEM did not interfere with the inhibitory effect of SCH772984 on phosphorylated ERK (pERK). Collectively, our studies suggest that combination therapy with GEM and SCH772984 effectively reduced PDAC cell viability and growth, and co-administration of NP encapsulated GEM and SCH772984 in separate NP systems is an effective treatment strategy for PDAC.

Keywords: ERK inhibitor, Gemcitabine, nanoparticle, PDAC

Cite this article: Nair G, *et al*. Extracellular Signal-Regulated Kinase Inhibitor SCH772984 Augments the Anti-Cancer Effects of Gemcitabine in Nanoparticle Form in Pancreatic Cancer Models. *International Journal of Molecular and Cellular Medicine. 2024; 13(3):220-233.*

*Corresponding: Gauthami G Nair
Address: Department of Biological Sciences, NDSU.
E-mail: gauthami.nair@ndsu.edu

© The Author(s).
Publisher: Babol University of Medical Sciences
This work is published as an open access article distributed under the terms of the Creative Commons Attribution 4.0 License (http://creativecommons.org/licenses/by-nc/4). Non-commercial uses of the work are permitted, provided the original work is properly cited.

[Downloaded from ijmcmed.org on 2026-11-14]

[DOI: 10.22088/IJMCM.BUMS.13.3.220]

Introduction

PDAC, a cancer of the exocrine glands, is responsible for over 90% of pancreatic cancer cases. It has a dismal 5-year survival rate of only 13% making it a highly lethal disease (1, 2). While surgical resection remains one of the treatment strategies, it is limited to only about 15-20% of the patients because of distant metastases, involvement of pivotal vasculature, and impacts on digestion and metabolism post-surgery (1). Thus, regardless of suitability for surgical intervention, most patients undergo chemotherapy. Current choices are FOLFIRINOX (5-fluorouracil, leucovorin, irinotecan, oxaliplatin) and gemcitabine (GEM) with a nanoparticle-encapsulated version of paclitaxel (nab-paclitaxel). While the former results in an increased overall survival, it is also associated with increased toxicity (3, 4). On the other hand, GEM with nab-paclitaxel has shown to increase survival time compared to treatment with GEM alone (5, 6); however, a downside to GEM-based therapy is that PDAC cells develop rapid resistance to it. Hence, there is a compelling need to identify agents that would enhance GEM's effects for PDAC treatment.

Over 95% of PDAC tumors have an oncogenic Kirsten rat sarcoma viral oncogene homologue (*KRAS)* mutation (commonly G12D, G12V, and G12R) leading to sustained and uncontrolled growth promotion that drives the progression of the disease (7). Hence, strategies to inhibit hyperactive *KRAS* signaling through direct or indirect approaches have been heavily pursued. Direct targeting of *KRAS* has been challenging resulting in few leads; however, a new clinical trial using a *KRAS* G12D inhibitor (MRTX1133) is underway. Indirect approaches targeting downstream *KRAS* effectors such as rapidly accelerated fibrosarcoma (RAF) and mitogen-activated protein kinase (MEK) have been stymied due to compensatory reactivation of this pathway (8). Thus, an alternate approach is targeting this pathway further downstream with the use of ERK inhibitors (9, 10) . First generation ERK inhibitors showed disappointing results in clinical trials as they do not bring any conformational change to ERK1/2 upon binding and resulted in subsequent reactivation of ERK by MEK. Thus, new ERK inhibitors such as SCH772984 were developed, which have a dual mechanism of inhibiting ERK1/2 and simultaneously bringing a conformational change to its structure preventing further activation by MEK1/2 (11).

For any combination therapy to be effective, the agent must be solubilized, accumulate in the tumor microenvironment, and synergize to reduce tumor cell growth (12). Both GEM and SCH772984 have limited utility in the free form due to relatively rapid clearance and solubility issues, respectively. GEM is rapidly metabolized by cytidine deaminase to inactive 2', 2'-difluoro-deoxyuridine (dFdU) and cleared from the system (13). SCH772984 is highly hydrophobic, which makes developing an effective formulation challenging. NP technologies are well-established platforms for augmenting the systemic half-life of drugs and modulating aqueous solubility. As such, NP can stabilize encapsulated drugs against non-specific biochemical degradation, and mitigate side effects *via* controlling drug release. Therefore, encapsulation of an enzyme-sensitive drug such as GEM within a NP has been reported as a viable strategy to control its plasma half-life. At the same time, encapsulation of SCH772984 within nanoscale particles can provide an opportunity to regulate its biodistribution, drug release, and non-specific tissue accumulation. Many studies have adopted NP strategies to encapsulate drug components of combination therapy, demonstrating augmented efficacy of the formulation in controlling cancer growth, both *in vitro* and *in vivo* (6, 14, 15). In most of the studies, combination therapies are usually encapsulated within a single NP. One unresolved

[Downloaded from ijmcmed.org on 2026-11-14]

[DOI: 10.22088/IJMCM.BUMS.13.3.220]

mechanistic question, particularly from a formulation standpoint, that remains unanswered is whether co-administration of drugs encapsulated in separate nanoparticles (a two-nanoparticle system), each of which encapsulates a particular candidate for combination therapy, will be a viable approach compared to administering the drugs in their free form. In this report, we aimed to tackle this fundamental question. We hypothesize that co-administration of NP formulations, which individually encapsulate unique drugs, will provide a facile opportunity to regulate effective drug concentrations *in vitro* and will provide augmented cellular effects of drugs. We aimed to test this hypothesis using our established NP platform, composed of poly (ethylene glycol)-b-poly (carbonate)-based block copolymer (PEG-PC) appended with pH-sensitive tertiary amine side chains (8, 16). Termed PEG-PC nanoparticles, the uniqueness of this platform is the fact that the NP can stabilize the encapsulated drug at pH 7.4 (plasma pH) and promote drug release in an acidic pH, ranging from pH 4.5-6 (8). This property of PEG-PC nanoparticles renders the platform particularly suitable for drug delivery in PDAC where the pH is in the acid range. Therefore, we used these PEG-PC nanoparticles to encapsulate GEM or SCH772984, and subject proliferating PDAC cells to these formulations, either in free or encapsulated form simultaneously, to distinguish, compare, and contrast the relative efficacy of the individual drugs against PDAC cells as part of continual mechanistic studies of our earlier published report (8, 14, 17). We envision that the data generated from this project will provide mechanistic insight related to formulation-associated variables of NP-based cancer therapy.

Materials and methods

Nanoparticle Formulations

The synthesis and development of NP formulations consisting of SCH772984, an ERK inhibitor, and GEM used in this manuscript have been developed earlier by Ray et al (8). Briefly, these particles are composed of poly (ethylene glycol)-b-poly (carbonate)-based block copolymers, where the poly (carbonate) block was appended with 2-pyrrolidin-1-yl-ethyl-amine and N, N′-dibutylethylenediamine (DBA) side chains. For co-administration, we encapsulated GEM and SCH772984 separately in these nanoparticles. While GEM was encapsulated *via* chemically linking it to the poly (carbonate) block, SCH772984 was physically entrapped within the polymeric particles. The NP was tested for their particle size, i.e., hydrodynamic diameter, surface charge, and polydispersity index before and after drug loading (8). The NP formulations were stored at 4°C to minimize colloidal instability. The quantity of encapsulated drugs in NP formulations was calculated from UV-Vis spectroscopic studies.

Cell Viability Assay

Two PDAC cell lines, MIA PaCa-2 and PANC-1 cells, were seeded (3,000 cells/well) in 96-well plates and allowed to grow until they reached 70-80% confluency. The cells were then treated with 1 µM of unencapsulated or separately encapsulated GEM and SCH772984 for co-administration. While MIA PaCa-2 cells were treated with these formulations for 48 h and 72 h, PANC-1 cells were treated for 48 h and 96 h. After the treatment, cell viability was tested using MTT (3-(4, 5-dimethylthiazol-2-yl)-2, 5-diphenyl tetrazolium bromide) reagent. The cells were incubated with the reagent for 3 h at 37°C. DMSO was used to dissolve the formazan crystals in the well and absorbance was measured at 570 nm. The graphs (Figure 1) are representative of the average % viability ± standard deviation from three biological replicates.

[Downloaded from ijmcmed.org on 2026-11-14]

[DOI: 10.22088/IJMCM.BUMS.13.3.220]

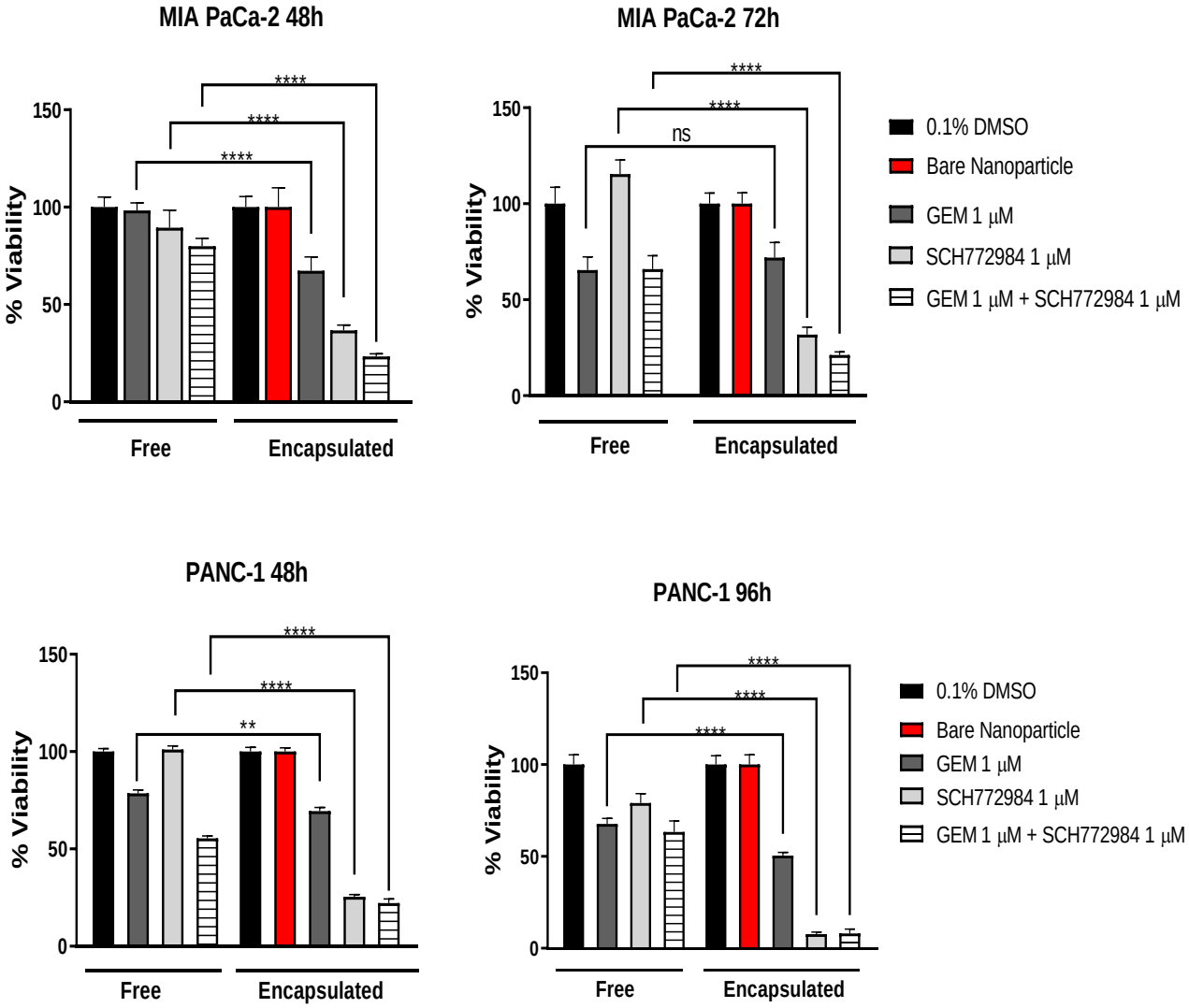

Fig. 1. Effect of GEM, SCH772984, and their combination in free and encapsulated forms on *in vitro* cell viability of MIA PaCa-2 and PANC-1 cell lines over time. MIA PaCa-2 and PANC-1 cells (3,000 cells/well of a 96-well plate) were treated with 1 μM of GEM, SCH772984, and their combination in the free and individually encapsulated forms for 48, 72, or 96 h. The graphs are representative of the averages ± standard deviations from three biological replicates for each cell line.

Matrigel Growth Assay

Corning® Matrigel® (50 μL/well) was placed at the bottom of a 48-well plate, and the plate was incubated at 37°C for 30 minutes to allow the Matrigel to solidify. MIA PaCa-2 cells were then seeded on the Matrigel at a seeding density of 4,000 cells/well. The cells were allowed to grow for 48 h and were treated with the following treatment groups: unencapsulated and encapsulated SCH772984 (0.1 μM), unencapsulated and encapsulated GEM (1 μM), and unencapsulated and encapsulated SCH772984 and GEM administered together (2 NP system) at 0.1 μM and 1 μM, respectively. Control cells were treated with either 0.1% DMSO or bare nanoparticles (not drug loaded). The representative images of the cell colonies for each treatment were taken after 4 days. Figure 2 is a representative image from three biological replicates.

[Downloaded from ijmcmed.org on 2026-11-14]

[DOI: 10.22088/IJMCM.BUMS.13.3.220]

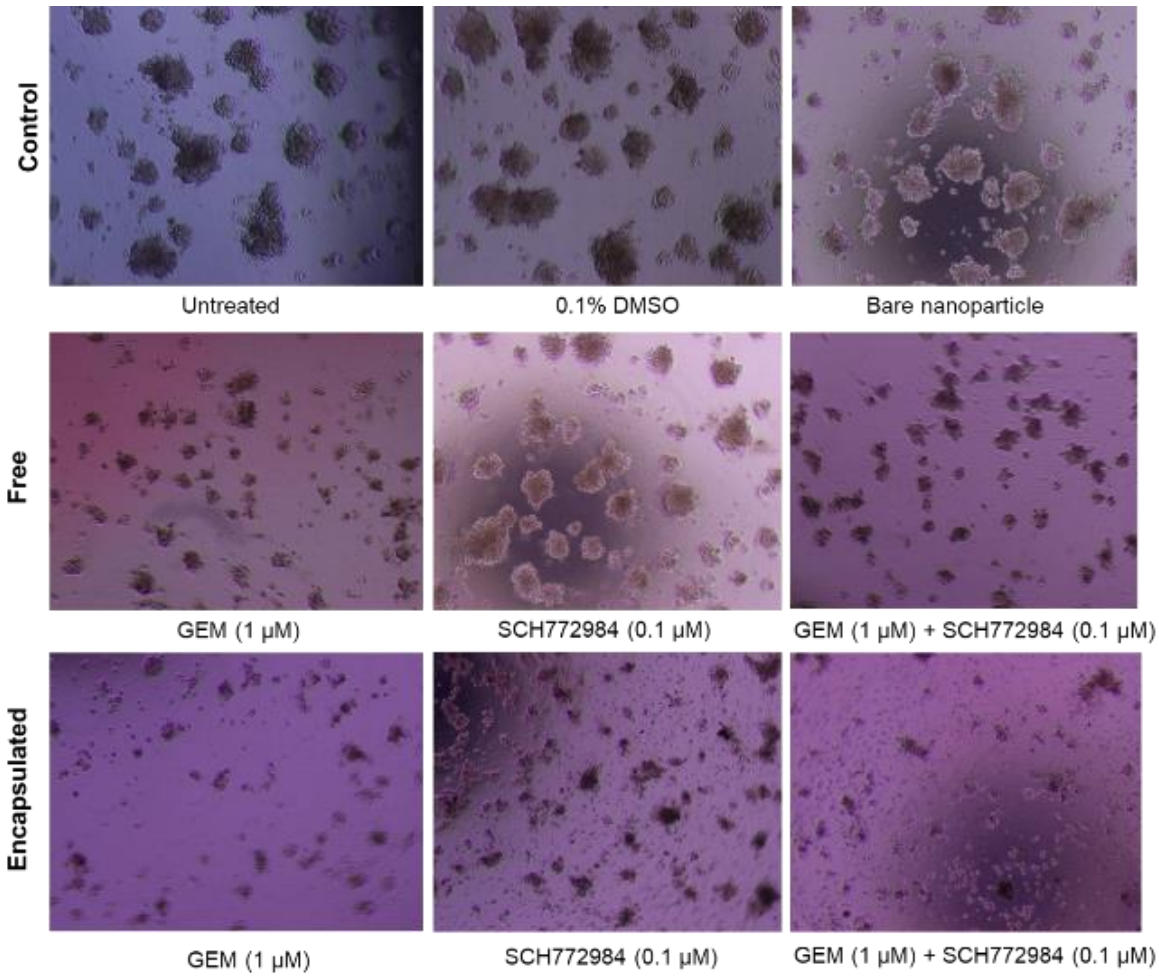

Fig. 2. Effect of GEM, SCH772984 and their combination in free and encapsulated forms on PDAC growth on Matrigel. MIA PaCa-2 cells (4,000 cells/well grown on a layer of Matrigel were treated with free and encapsulated SCH772984 (0.1 µM, free and encapsulated GEM (1 µM), and free and encapsulated SCH772984 and GEM administered together at 0.1 µM and 1 µM, respectively. The images of the colony size of the tumor cells, taken after 4 days of treatment, are representative of three biological replicates.

Western Blot Experiments

To reveal the protein-level interactions of NP-encapsulated GEM and SCH772984 compared to their standard form, we conducted western blot analysis. MIA PaCa-2 and PANC-1 cells (200,000 cells/well) were treated with 5 µM of unencapsulated and encapsulated SCH772984, 10 µM of unencapsulated and encapsulated GEM, and a combination of 5 µM SCH772984 and 10 µM GEM in their unencapsulated and encapsulated forms. Additionally, appropriate controls such as an untreated cell control, DMSO control (vehicle), and bare nanoparticle control were also included. After 1, 6, 12 and 24 h time points, cell lysates were collected by scraping using a cell lysis buffer along with 100X protease/phosphatase inhibitor cocktail (Cell Signaling Technology). The cell lysates were centrifuged at 13000 rpm for 15 minutes at 4°C. The supernatant was collected after centrifugation and protein estimation was performed using a BCA kit (Thermo Scientific). Based on the protein concentration, 20 µg of protein was loaded into a 10% SDS gel.

[Downloaded from ijmcmed.org on 2026-11-14]

[DOI: 10.22088/IJMCM.BUMS.13.3.220]

The gels were run at 100 V for 2 h using tris glycine buffer. Once the protein bands were separated on the gel, they were transferred onto a 0.2 μm nitrocellulose membrane. The transfer was carried out at 100 V for 70 minutes. Following the transfer, the blots were blocked in 5% bovine serum albumin blocking buffer for 2.5 h. The blocking buffer, primary antibodies and secondary antibodies (Cell Signaling Technology) were prepared in 1X Tris buffer supplemented with Tween-20. The proteins: phosphorylated ERK (pERK) and total ERK (tERK) were detected by using the following primary antibodies (1:1000) - phospho-p44/42 MAPK (ERK 1/2) (Thr202/Tyr204) and total p44/42 MAPK (ERK 1/2). The secondary antibody (1:2000) used was anti-rabbit IgG, HRP-linked antibody along with anti-biotin, HRP-linked antibody (1:5000). SuperSignal West Femto Maximum Sensitivity Substrate (Thermo Scientific) was used to detect the bands. The images are representative of three biological replicates.

PDX *Ex-vivo* Explant Study

PDX tumor tissue pieces of human PDAC origin: patient A20 (Male, 59-years old) and patient A22 (Female, 61-years old), obtained from NOD scid gamma (NSG) immunodeficient mice were used for an *ex-vivo* explant study. The tumor grade was 'moderately differentiated' to 'well differentiated' in A20 and A22, respectively. Additionally, the tumor stage ranged from stage two to three and was collected from mouse generations F2 (A20) and F4 (A22). The tumor tissue of dimension 2-3 mm^3 was placed in a 24-well plate precoated with Matrigel and treated with 10 μM GEM and 2 μM SCH772984 in their free and encapsulated forms, individually and in combination for 72 h. The tissue samples were supplemented with high-glucose DMEM containing 10% FBS and 1× antibiotic/antimycotic solution along with 0.01 mg/mL insulin, 0.01 mg/mL hydrocortisone, and 5 mM GlutaMAX. After 72 h, the tissue was fixed in formalin and processed using conventional histology protocol. 5 μm microtome sections of the embedded tissue chunks were stored at 4°C until further use. The animal experimental procedures involving the use of PDX tissue sections were approved by North Dakota State University's (NDSU) Institutional Animal Care and Use Committee (protocol number: IACUC20220077). Additionally, NDSU is registered with the United States Department of Agriculture as an Animal Research Facility (45-R-002) and an Animal Welfare Assurance (A3244-01) with the National Institute of Health- Office of Laboratory Animal Welfare (OLAW).

Immunohistochemistry

Tumor tissue slides were deparaffinized at 60 °C for 2 h and subjected to xylene treatment followed by rehydration using decreasing gradients of ethanol prepared in water. The rehydrated tissue sections then underwent antigen retrieval where the slides were immersed in Tris-EDTA buffer (pH 9.0) kept at 95 °C for 30 minutes. The sections were stained using a primary antibody: Ki-67 recombinant rabbit monoclonal antibody (SP6) (Invitrogen MA5-14520) at a concentration of 1:200 overnight at 4 °C. Subsequently, Ki-67 was detected using a secondary anti-rabbit goat Alexa Fluor 488 antibody (Invitrogen A11034) at a concentration of 1:250 at room temperature. Later, nuclei were stained using DAPI and the slides were mounted in VECTASHIELD. The images were taken at 5X magnification and processed using the ImageJ software.

H&E Staining

Tumor tissue slides were deparaffinized at 60 °C for 2 h and immersed in xylene and ethanol gradients to remove the paraffin wax. The rehydrated tissue sections were then stained using hematoxylin for 8 minutes

[Downloaded from ijmcmed.org on 2026-11-14]

[DOI: 10.22088/IJMCM.BUMS.13.3.220]

and counterstained using eosin. After the staining procedure, the slides were subjected to dehydration. The rinsed and cleared slides were mounted using Cytoseal mounting medium, and images were taken at 5x magnification. Image processing was done using the ImageJ software.

Statistical Analysis

Experiments in Figures 1-3 were performed in triplicate. The data are represented as the average of the replicates ± standard deviation. A student's t-test was performed to determine statistical significance (p-value < 0.05).

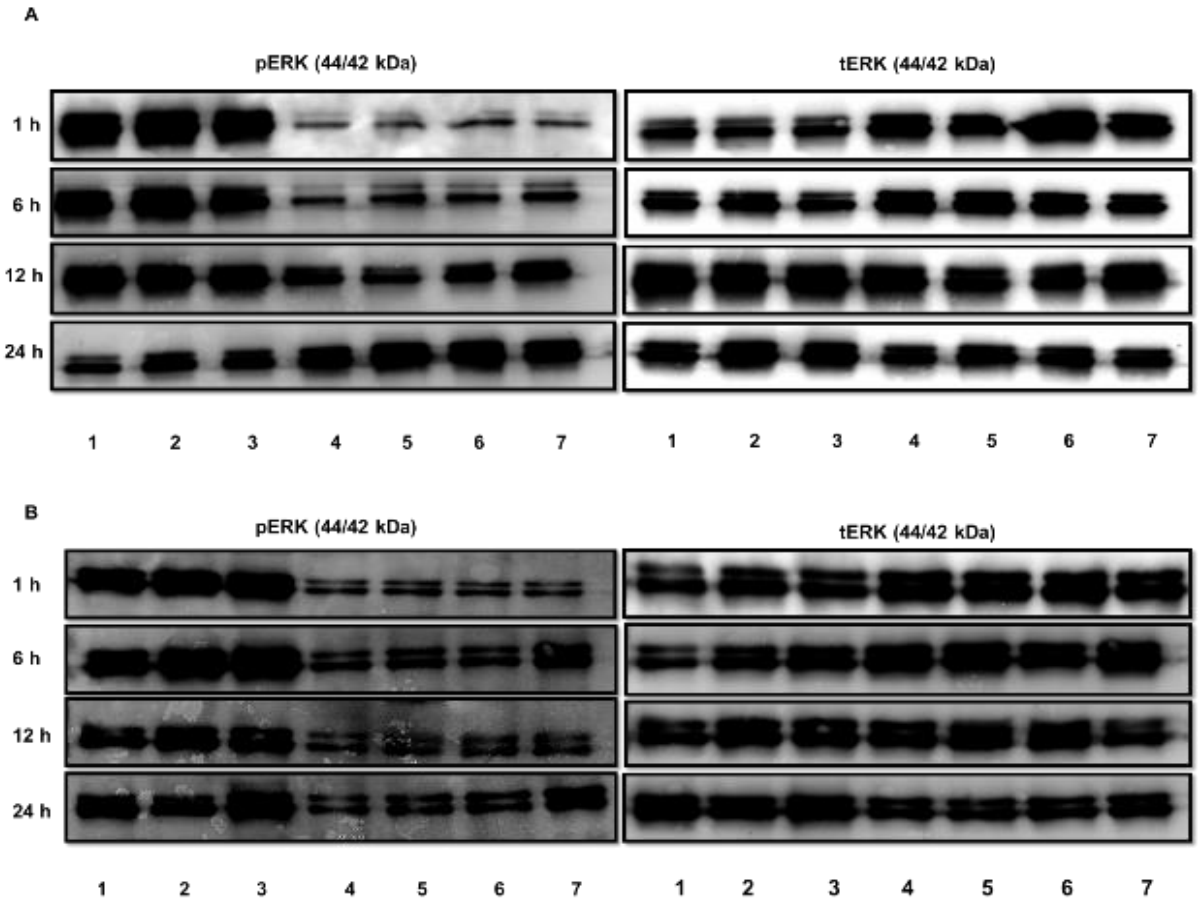

Fig. 3. Western blots showing the effect of GEM +/- SCH772984 in free and co-administered forms on ERK protein activity and expression. MIA PaCa-2 (A.) and PANC-1 (B.) cells grown in 6-well plates (200,000 cells/well) were treated with 5 µM SCH772984 in its free and encapsulated form, and in combination with 10 µM GEM in its free and encapsulated form for 1h, 6h, 12h and 24h. The protein lysates were collected and phosphorylated ERK (pErk) and total ERK (tErk) levels were determined. **1:** cell control, **2:** 0.1% DMSO control, **3:** bare nanoparticle control, **4:** free SCH772984, **5:** encapsulated SCH772984, **6:** free GEM + free SCH772984 and **7:** encapsulated GEM + encapsulated SCH772984. These images are representative of three biological replicates.

Results

SCH772984 potentiates the anti-proliferative effects of GEM, particularly in the NP form

[Downloaded from ijmcmed.org on 2026-11-14]

[DOI: 10.22088/IJMCM.BUMS.13.3.220]

MTT assays (Figure 1) were done to assess the effects of the unencapsulated and NP-encapsulated forms of the drugs (GEM and SCH772984 at 1 μM each) on cell viability across two PDAC cell lines: MIA PaCa-2 and PANC-1. Free or unencapsulated forms of GEM or SCH772984 alone or in combination reduced PDAC viability by at most 50%. Remarkably, NP encapsulated drugs, when administered simultaneously (co-administered), reduced PDAC viability by up to 90%. Adding SCH772984 to GEM in a NP-encapsulated form enhanced the cytotoxicity compared to GEM alone. These results suggest that SCH772984 potentiates the cytotoxic effects of GEM and that GEM and SCH772984 co-administered in separate NP systems is highly effective at killing PDAC cells. We used asterisks to denote statistical significance using an unpaired t-test where, **** = $p < 0.0001$, ** = $p < 0.01$ and ns = not significant.

Encapsulated SCH772984 enhances the cytotoxic effects of GEM in a 3-D model

To mimic an *in vivo* environment, PDAC cell growth assays using the extracellular basement membrane extract, Matrigel, were performed with MIA PaCa-2 cells. Cells were treated for 4 days with 0.1 μM and 1 μM of SCH772984 and GEM, respectively, or the two agents were co-administered, in their unencapsulated and encapsulated forms. All treatments were compared with three controls: (1) untreated cells, (2) 0.1% DMSO, and (3) bare nanoparticle (with no drug). Cells treated with the free forms of the drugs, or their combination, showed reduced colony size compared to the controls. However, cells treated with the encapsulated forms of the drugs resulted in smaller colonies compared to that formed from the treatment with controls and the unencapsulated combination (Figure 2). Furthermore, the cells co-administered with encapsulated GEM and encapsulated SCH772984 showed the least amount of growth compared to the free form of the co-treatment. The Matrigel growth assay demonstrated that, while the combination of GEM and SCH772984 was more effective at reducing colony growth than either of the drug alone, the combination in encapsulated form was more effective in their encapsulated forms compared to the free forms.

Free and encapsulated SCH772984 inhibits pERK signaling in PDAC cells

To determine if the free and encapsulated forms of SCH772984 can engage their intended protein target and there is no interference upon co-administration of GEM (or NP-bound GEM), western blotting for pERK was performed. As expected, MIA PaCa-2 cells treated with SCH772984 (5 μM) in unencapsulated (lane 4) and encapsulated (lane 5) forms showed a large reduction in pERK protein expression at 1 h and 6 h (Figure 3A). ERK phosphorylation was restored between 12 h - 24 h. When GEM (10 μM) was added to SCH772984 in either the free (lane 6) or encapsulated (lane 7) forms, there was no change in pERK expression in MIA PaCa-2 cells. Similarly, SCH772984 in free and encapsulated forms reduced pERK expression in PANC-1 cells with no effect of added GEM. Although pERK reduction in SCH772984-treated PANC-1 cells was not as prominent as in MIA PaCa-2 cells, it was more sustained (Figure 3B). The tERK protein levels were the same across the controls and treatments, reestablishing that SCH772984 affects phosphorylation of ERK 1/2 and not global protein levels. Collectively, these results suggest SCH772984 inhibited its target, ERK 1/2, for both unencapsulated and encapsulated forms in both PDAC cell lines. Additionally, the presence of GEM and polymeric nanoparticles did not abrogate the effects of SCH772984 on ERK 1/2 phosphorylation.

Effect of SCH772984 and GEM on Ki-67 in PDX PDAC model

To reveal if nanoparticles can diffuse into tissue sections *ex vivo*, and affect Ki-67 cell proliferation marker, PDX PDAC tissues (Patients A20 and A22) obtained from F2 and F4 generations, respectively, were

[Downloaded from ijmcmed.org on 2026-11-14]

[DOI: 10.22088/IJMCM.BUMS.13.3.220]

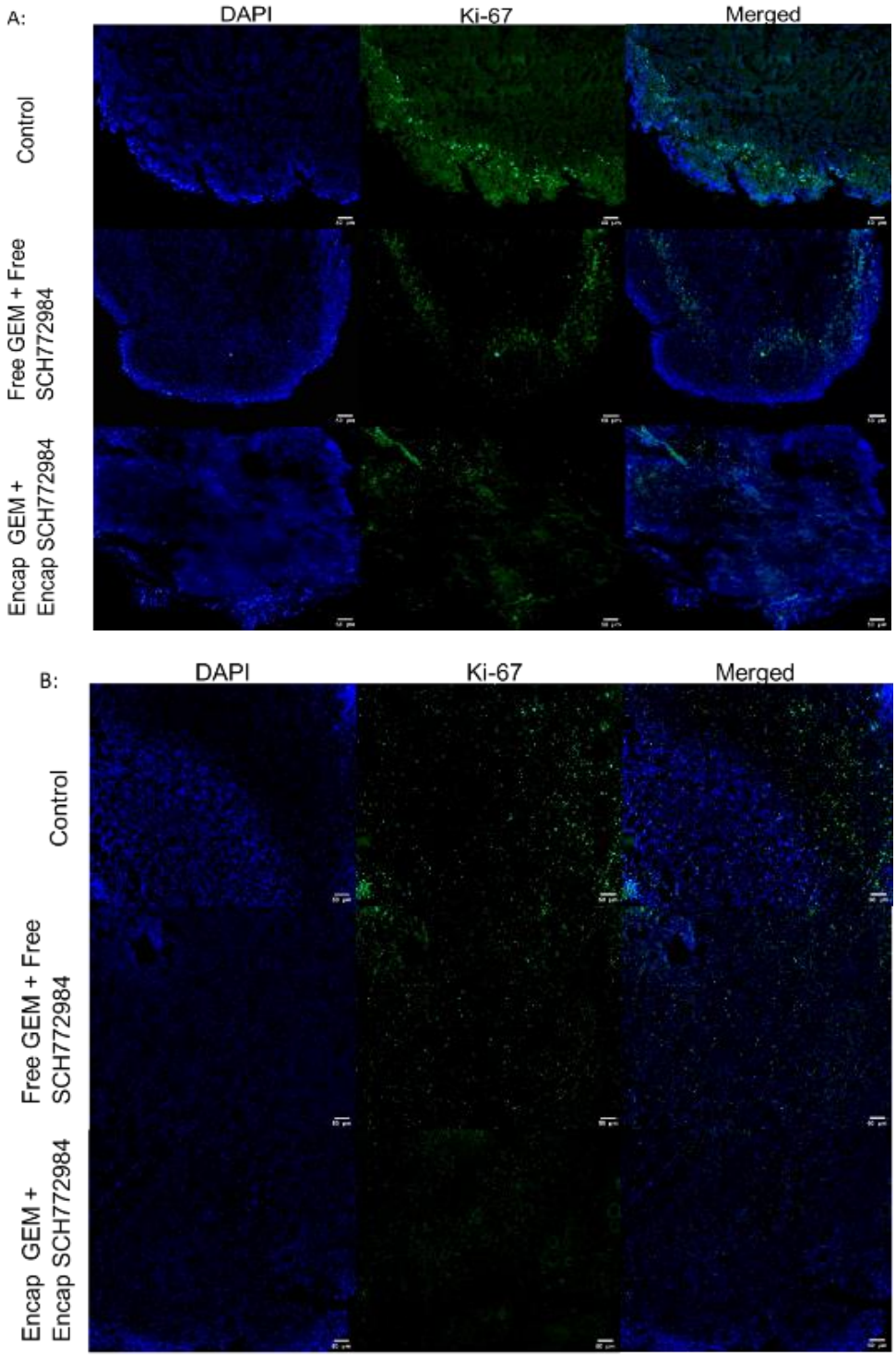

Fig. 4. Ki-67 immunostaining showing the effect of GEM, SCH772984 and its combination in the co-administered form on the cell proliferation marker in a patient derived xenograft (PDX) model of PDAC. 2-3 mm^3 PDX tumor chunks were treated with 10 µM GEM and 2 µM SCH772984 in its free and encapsulated form. The formalin-fixed and paraffin embedded tissue blocks were cut into tissue sections for Ki-67 staining. The tissue sections (A: patient line A20 and B: patient line A22) treated with the combination of both the drugs visually appeared to have lesser number of Ki-67 cells compared to the control. The images were processed on ImageJ.

[Downloaded from ijmcmed.org on 2026-11-14]

[DOI: 10.22088/IJMCM.BUMS.13.3.220]

sliced into smaller tumor pieces with dimension of 2-3 mm^3. The tumor pieces were treated with 10 μM GEM and 2 μM SCH772984 in their free and encapsulated forms, individually and in combination for 72 h. Post treatment, the explants were fixed in formalin and paraffin embedded to be cut into 5 μm sections using a microtome. The sections were then stained for a cell proliferation marker, Ki-67 (Figure 4; A: patient line A20 and B: patient line A22). Tumor pieces that received a combination of encapsulated GEM and encapsulated SCH772984, showed a qualitative reduction in Ki-67 positive cells (green signal) compared to the control and the tissue treated with free GEM and free SCH772984. These results suggest that the combination of GEM and SCH772984 is more effective in their encapsulated form than in its free form at reducing cell proliferation.

Effect of SCH772984 and GEM on tissue architecture in PDX PDAC model

PDX PDAC tumor pieces were harvested from mice and treated with 10 μM GEM and 2 μM SCH772984 in unencapsulated and encapsulated forms, individually and in combination for 72 h. After treatment, the formalin-fixed tissues were paraffin embedded and cut into 5 μm sections. The sections were then used for H & E staining (Figure 5; A: patient line A20 and B: patient line A22) to investigate the integrity of the tissue architecture. The images reveal PDAC tissue characteristics such as abundant stroma and irregularly shaped glands. H & E staining showed that the tissue architecture remained the same across all treatments compared to the control and that the nanoparticles did not affect the tissue integrity. It is possible that the treatment duration was too short to observe any significant changes in tumor cell clusters between tissues treated with SCH772984, GEM, and its combination. We are currently pursuing further experiments to confirm our hypothesis.

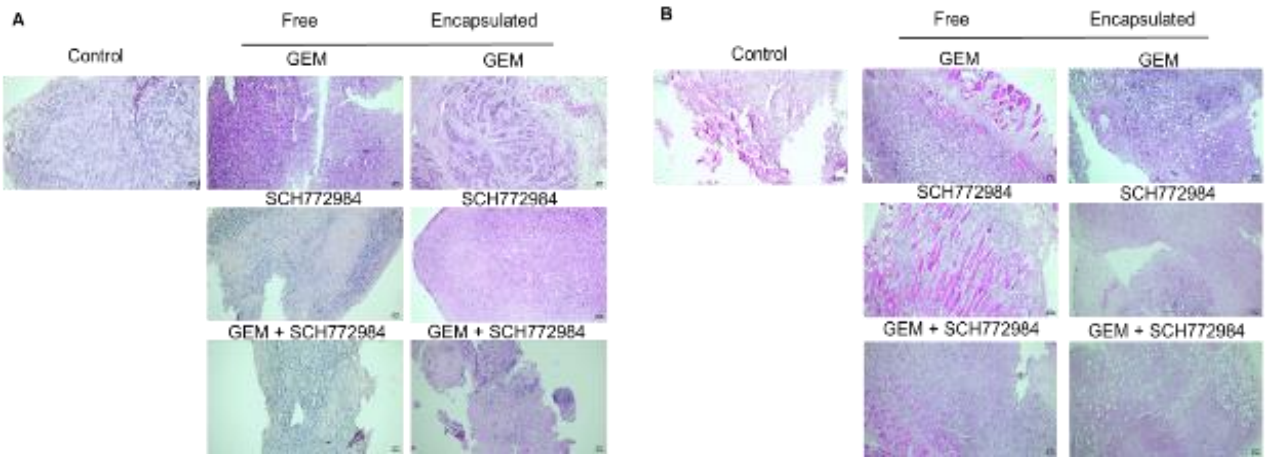

Fig. 5. H&E staining showing the effect of GEM, SCH772984 and its combination in the co-administered form on tissue architecture in a patient derived xenograft (PDX) model of PDAC. 2-3 mm^3 PDX tumor chunks were treated with 10 μM GEM and 2 μM SCH772984 in its free and encapsulated form. The formalin-fixed and paraffin embedded tissue blocks were cut into tissue sections for H & E staining. The tissue sections (A: patient line A20 and B: patient line A22) showed characteristics of PDAC and the tissue architecture remained intact after the treatments.

[Downloaded from ijmcmed.org on 2026-11-14]

[DOI: 10.22088/IJMCM.BUMS.13.3.220]

Discussion

Although GEM by itself has been used for decades as a leading chemotherapy for PDAC patients (18-20), the inherent and acquired resistance to GEM (21, 22) has prompted the search for synergistic anti-cancer agents to enhance tumor cell death. Here, we combined SCH772984, an ERK inhibitor, with GEM in their unencapsulated and encapsulated forms and determined their effects on PDAC cell proliferation and cell signaling. Our results show that SCH772984 potentiates the anti-proliferative effects of GEM in PDAC cell models, and this effect is enhanced when the two drugs are co-administered in nanoparticle-encapsulated systems. We observed that encapsulating the drugs separately in PEG-PC nanoparticles, and co-administering the NP formulations, to achieve the desired concentration of GEM and SCH772984 resulted in the highest reduction of cell viability for MIA PaCa-2 and PANC-1 type PDAC cell lines at all-time points.

KRAS mutations occur in up to 90% of PDAC patients, with the most common mutations occurring at codon 12 (G12D, G12V, and G12R; (23-27)). *KRAS* mutations triggers a highly aggressive phenotype through activation of downstream signaling pathways such as mitogen-activated protein kinase (*MAPK)* and phosphoinositide-3-kinase (*PI3K)* pathways (24). Thus, significant efforts have been made to directly (7, 28) or indirectly target KRAS signaling in PDAC (29-31), but compensatory reactivation of KRAS signaling has reduced efficacy of these approaches (8). Here, we used a second-generation ERK 1/2 inhibitor, SCH772984, that causes a conformation change that prevents its reactivation.

It is critical that targeted therapies, like an ERK inhibitor, are able to block their intended target when combined with additional drugs or when packaged within nanoparticulated systems. Here, we demonstrated that NP SCH772984 was just as effective at inhibiting pERK expression as the free form of the drug, and combination with GEM did not attenuate this effect similar to earlier studies (10). Analogous to our earlier observations, MIA PaCa-2 cells, which harbor a $KRAS^{G12C}$ mutation were found to be more sensitive to the ERK inhibitor than PANC-1 cells, which harbor a $KRAS^{G12D}$ mutation. Tumor explant studies showed that the combination of GEM and SCH772984 in their unencapsulated and encapsulated forms did not affect PDAC tumor architecture, indicating treatment-related cellular damage, or reduction of tumor cell clusters. A plausible explanation for this could be that the treatment period was not long enough (only 3 days), which was a shorter duration compared to other *ex-vivo* studies (32, 33). However, Ki-67 staining of the tissue sections from the same *ex-vivo* study showed that there was a qualitative reduction in the Ki-67 positive cells in the tissue sections treated with co-administered NP formulations of SCH772984 and GEM. These results suggest that co-administration of GEM and SCH772984 is an effective combination to prevent PDAC proliferation that is driven by KRAS signaling.

GEM has been combined with several other treatment approaches including nab-paclitaxel (6), the epidermal growth factor receptor inhibitor erlotinib (34), and the MEK inhibitor trametinib (35). While these combinations showed a significant increase in overall survival in patients compared to GEM alone, these combinations carry associated side effects emphasizing the importance of seeking other anti-cancer agents suitable for combination with GEM and additional drug delivery approaches. Our results suggest an ERK inhibitor could be used in combination with GEM for more effective treatment of PDAC.

The ability of nanoparticles to increase drug stability, solubility, and accumulation at the tumor site makes this drug delivery approach attractive for GEM-based combination therapy for PDAC patients. The

[Downloaded from ijmcmed.org on 2026-11-14]

[DOI: 10.22088/IJMCM.BUMS.13.3.220]

challenges arising from the off-target toxicity of GEM and high hydrophobicity of SCH772984 can be addressed through the utilization of NP formulations. By encapsulating these compounds in NP, we improve their pharmacokinetic and pharmacodynamic characteristics. The results from this study are consistent with our prior observations (8), where the NP-encapsulated drugs reduced cell proliferation more than the free forms of the drugs for PDAC cell lines. However, here, we further show that co-administration is superior to co-encapsulation. Co-administered systems are advantageous because the individual drug dosages and administration timing can be regulated independently (36), as seen in our PEG-PC nanoparticles containing SCH772984 and GEM. Furthermore, a plausible reason for co-administration to work better than free form of the drugs is that the nanoparticles could be taken up by the cells *via* the endosomal pathway where the drug is released under acidic pH in the endosome (8, 37, 38).

Collectively, these results support further pre-clinical studies to evaluate the efficacy of NP formulations of SCH772984 in combination with GEM. Particularly, *in-vivo* studies are needed to determine the pharmacokinetics and therapeutic benefits of NP GEM and SCH772984 in PDAC models.

References

1. Hatzivassiliou G, Liu B, O'Brien C, et al. ERK Inhibition Overcomes Acquired Resistance to MEK Inhibitors. Mol Cancer Ther 2012;11:1143-54.

2. Halbrook CJ, Lyssiotis CA, Pasca di Magliano M, et al. Pancreatic cancer: Advances and challenges. Cell 2023;186:1729-54.

3. Sarantis P, Koustas E, Papadimitropoulou A, et al. Pancreatic ductal adenocarcinoma: Treatment hurdles, tumor microenvironment and immunotherapy. World J Gastrointest Oncol 2020;12:173-81.

4. Berger AK, Haag GM, Ehmann M, et al. Palliative chemotherapy for pancreatic adenocarcinoma: a retrospective cohort analysis of efficacy and toxicity of the FOLFIRINOX regimen focusing on the older patient. BMC Gastroenterol 2017;17:143.

5. de Jesus VHF, Camandaroba MPG, Donadio MDS, et al. Retrospective comparison of the efficacy and the toxicity of standard and modified FOLFIRINOX regimens in patients with metastatic pancreatic adenocarcinoma. J Gastrointest Oncol 2018;9:694-707.

6. Blomstrand H, Scheibling U, Bratthäll C. Real world evidence on gemcitabine and nab-paclitaxel combination chemotherapy in advanced pancreatic cancer. BMC Cancer 2019;19:40.

7. Von Hoff DD, Ervin T, Arena FP, et al. Increased survival in pancreatic cancer with nab-paclitaxel plus gemcitabine. N Engl J Med 2013;369:1691-703.

8. Huang L, Guo Z, Wang F, et al. KRAS mutation: from undruggable to druggable in cancer. Signal Transduct Target Ther 2021;6:386.

9. Ray P, Nair G, Ghosh A, et al. Microenvironment-sensing, nanocarrier-mediated delivery of combination chemotherapy for pancreatic cancer. J Cell Commun Signal 2019;13:407-20.

10. Hayes TK, Neel NF, Hu C, et al. Long-Term ERK Inhibition in KRAS-Mutant Pancreatic Cancer Is Associated with MYC Degradation and Senescence-like Growth Suppression. Cancer Cell 2016;29:75-89.

11. Kidger AM, Munck JM, Saini HK, et al. Dual-Mechanism ERK1/2 Inhibitors Exploit a Distinct Binding Mode to Block Phosphorylation and Nuclear Accumulation of ERK1/2. Mol Cancer Ther 2020;19:525-39.

12. Li J, Burgess DJ. Nanomedicine-based drug delivery towards tumor biological and immunological microenvironment. Acta Pharm Sin B 2020;10:2110-24.

[Downloaded from ijmcmed.org on 2026-11-14]

[DOI: 10.22088/IJMCM.BUMS.13.3.220]

13. Ciccolini J, Serdjebi C, Peters GJ, et al. Pharmacokinetics and pharmacogenetics of Gemcitabine as a mainstay in adult and pediatric oncology: an EORTC-PAMM perspective. Cancer Chemother Pharmacol 2016;78:1-12.

14. Ray P, Dutta D, Haque I, et al. pH-Sensitive Nanodrug Carriers for Codelivery of ERK Inhibitor and Gemcitabine Enhance the Inhibition of Tumor Growth in Pancreatic Cancer. Mol Pharm 2021;18:87-100.

15. Smith RC, Bulanadi JC, Gill AJ, et al. Pancreatic adenocarcinoma preferentially takes up and is suppressed by synthetic nanoparticles carrying apolipoprotein A-II and a lipid gemcitabine prodrug in mice. Cancer Lett 2020;495:112-22.

16. Engler AC, Chan JMW, Coady DJ, et al. Accessing New Materials through Polymerization and Modification of a Polycarbonate with a Pendant Activated Ester. Macromolecules 2013;46:1283-90.

17. Ray P, Kale N, Quadir M. New side chain design for pH-responsive block copolymers for drug delivery. Colloids Surf B Biointerfaces 2021;200:111563.

18. Burris HA, Moore MJ, Andersen J, et al. Improvements in survival and clinical benefit with gemcitabine as first-line therapy for patients with advanced pancreas cancer: a randomized trial. J Clin Oncol 1997;15:2403-13.

19. Colucci G, Giuliani F, Gebbia V, et al. Gemcitabine alone or with cisplatin for the treatment of patients with locally advanced and/or metastatic pancreatic carcinoma: a prospective, randomized phase III study of the Gruppo Oncologia dell'Italia Meridionale. Cancer 2002;94:902-10.

20. Oettle H, Arnold D, Hempel C, et al. The role of gemcitabine alone and in combination in the treatment of pancreatic cancer. Anticancer Drugs 2000;11:771-86.

21. Amrutkar M, Gladhaug IP. Pancreatic Cancer Chemoresistance to Gemcitabine. Cancers (Basel) 2017;9.

22. Jia Y, Xie J. Promising molecular mechanisms responsible for gemcitabine resistance in cancer. Genes & Diseases 2015; 2:299-306.

23. Fan Z, Fan K, Yang C, et al. Critical role of KRAS mutation in pancreatic ductal adenocarcinoma. Transl Cancer Res 2018;7:1728-36.

24. Pirlog R, Calin GA. KRAS mutations as essential promoters of lymphangiogenesis via extracellular vesicles in pancreatic cancer. J Clin Invest 2022;132.

25. Saiki Y, Jiang C, Ohmuraya M, et al. Genetic Mutations of Pancreatic Cancer and Genetically Engineered Mouse Models. Cancers (Basel) 2021;14.

26. Sun H, Zhang B, Li H. The Roles of Frequently Mutated Genes of Pancreatic Cancer in Regulation of Tumor Microenvironment. Technol Cancer Res Treat 2020;19:1533033820920969.

27. Zhang Z, Zhang H, Liao X, et al. KRAS mutation: The booster of pancreatic ductal adenocarcinoma transformation and progression. Front Cell Dev Biol 2023;11.

28. Wang X, Allen S, Blake JF. Identification of MRTX1133, a Noncovalent, Potent, and Selective KRAS(G12D) Inhibitor. J Med Chem 2022;65:3123-33.

29. Degirmenci U, Wang M, Hu J. Targeting Aberrant RAS/RAF/MEK/ERK Signaling for Cancer Therapy. Cells 2020;9.

30. Grierson PM, Tan B, Pedersen KS, et al. Phase Ib Study of Ulixertinib Plus Gemcitabine and Nab-Paclitaxel in Patients with Metastatic Pancreatic Adenocarcinoma. Oncologist 2023;28:e115-e23.

31. Zhang J, Darman L, Hassan MS, et al. Targeting KRAS for the potential treatment of pancreatic ductal adenocarcinoma: Recent advancements provide hope (Review). Oncol Rep 2023;50.

32. Decker-Farrell AR, Ma A, Li F, et al. Generation and ex vivo culture of murine and human pancreatic ductal adenocarcinoma tissue slice explants. STAR Protoc 2023;4:102711.

[Downloaded from ijmcmed.org on 2026-11-14]

[DOI: 10.22088/IJMCM.BUMS.13.3.220]

33. Kokkinos J, Sharbeen G, Haghighi KS, et al. Ex vivo culture of intact human patient derived pancreatic tumour tissue. Sci Rep 2021;11:1944.

34. Moore MJ, Goldstein D, Hamm J, et al. Erlotinib plus gemcitabine compared with gemcitabine alone in patients with advanced pancreatic cancer: a phase III trial of the National Cancer Institute of Canada Clinical Trials Group. J Clin Oncol 2007;25:1960-6.

35. Kawaguchi K, Igarashi K, Miyake K, et al. MEK inhibitor trametinib in combination with gemcitabine regresses a patient-derived orthotopic xenograft (PDOX) pancreatic cancer nude mouse model. Tissue Cell 2018;52:124-8.

36. Gao Y, Tang M, Leung E, et al. Dual or multiple drug loaded nanoparticles to target breast cancer stem cells. RSC Advances 2020;10:19089-105.

37. Jurczyk M, Kasperczyk J, Wrześniok D, et al. Nanoparticles Loaded with Docetaxel and Resveratrol as an Advanced Tool for Cancer Therapy. Biomedicines 2022;10.

38. Khafaji M, Zamani M, Vossoughi M, et al. Doxorubicin/Cisplatin-Loaded Superparamagnetic Nanoparticles As A Stimuli-Responsive Co-Delivery System For Chemo-Photothermal Therapy. Int J Nanomedicine 2019;14:8769-86.

[Downloaded from ijmcmed.org on 2026-11-14]

[DOI: 10.22088/IJMCM.BUMS.13.3.220]